Cell Reports
Article

Age-Related Oxidative Stress Compromises Endosomal Proteostasis

Elvira S. Cannizzo,[1,5] Cristina C. Clement,[1] Kateryna Morozova,[1] Rut Valdor,[1] Susmita Kaushik,[2] Larissa N. Almeida,[1,6] Carlo Follo,[1,5] Ranjit Sahu,[1] Ana Maria Cuervo,[2,4] Fernando Macian,[1,4] and Laura Santambrogio[1,3,4,*]
[1]Department of Pathology
[2]Department of Developmental and Molecular Biology
[3]Department of Microbiology and Immunology
[4]Institute for Aging Research
Albert Einstein College of Medicine, Bronx, NY 10461, USA
[5]Present address: Department of Medical Sciences, University of Piemonte Orientale Medical School, Novara 28010, Italy
[6]Present address: Instituto de Biofísica Carlos Chagas Filho, Universidade Federal do Rio de Janeiro, Rio de Janeiro 21941-902, Brazil
*Correspondence: laura.santambrogio@einstein.yu.edu
http://dx.doi.org/10.1016/j.celrep.2012.06.005

SUMMARY

A hallmark of aging is an imbalance between production and clearance of reactive oxygen species and increased levels of oxidatively damaged biomolecules. Herein, we demonstrate that splenic and nodal antigen-presenting cells purified from aging mice accumulate oxidatively modified proteins with side-chain carbonylation, advanced glycation end products, and lipid peroxidation. Furthermore, we show that the endosomal accumulation of oxidatively modified proteins interferes with the efficient processing of exogenous antigens and degradation of macroautophagy-delivered proteins. In support of a causative role for oxidized products in the inefficient immune response, a decrease in oxidative stress improved the adaptive immune response to immunizing antigens. These findings underscore a previously unrecognized negative effect of age-dependent changes in cellular proteostasis on the immune response.

INTRODUCTION

Reactive oxygen species (ROS) are molecules in which the outer electron orbital holds one or two unpaired electrons. Among these, hydrogen ($H^{\cdot}$), hydroxyl radical ($OH^{\cdot}$), transition metals (copper and iron), oxygen ($O^{\cdot}$ and $RO^{\cdot}$), diatomic oxygen ($O_2^{\cdot}$, $H\,O_2^{\cdot}$, $R\,O_2^{\cdot}$), and its superoxide ($O_2^{\cdot -}$) are the most abundant species (Halliwell, 2009; Hamanaka and Chandel, 2010; Wellen and Thompson, 2010; Cannizzo et al., 2011). ROS are physiologically produced by all cells and mostly derived from leakage of the electron transport chain in mitochondria (Barja and Herrero, 2000; Dufour et al., 2000; Starkov et al., 2004; Lin and Beal, 2006; Chandel, 2010; Cannizzo et al., 2011). In inflammatory cells a second important source of ROS production is the "oxidative burst," where the NADPH oxidase complex catalyzes the formation of diatomic oxygen, and the enzymes myeloperoxidase and bromoperoxidase catalyze the formation of hypochlorite (ClO^{-}), hypochlorous acid (HOCl), and hypobromous acid (HOBr) as an innate immune mechanism to eradicate pathogens (Park, 2003; Cathcart, 2004; Klebanoff, 2005; Dale et al., 2008). Because ROS are unstable molecular species that can readily induce the nonenzymatic oxidation of biomolecules, cells are equipped with a series of enzymes that include different isoforms of superoxide dismutase, catalase, peroxiredoxin, and glutathione peroxidase, to readily dispose of ROS (Johnson and Giulivi, 2005; Roberts and Sindhu, 2009; Chandel, 2010; Haigis and Yankner, 2010; Wellen and Thompson, 2010; Cannizzo et al., 2011). In aging cells an imbalance due to increased ROS production and a decrease in the levels and activity of the ROS-converting enzymes leads to the nonenzymatic oxidation of proteins, carbohydrates, lipids, and nucleic acids, a process generally known as oxidative stress (Broadley and Hartl, 2008; Alexeyev, 2009; Halliwell, 2009; Roberts and Sindhu, 2009; Hamanaka and Chandel, 2010; Wellen and Thompson, 2010; Cannizzo et al., 2011; Durieux et al., 2011).

The mechanism(s) for clearance of oxidized proteins depends on the subcellular localization of the protein, the level of oxidation, and the nature of the specific oxidized amino acid. Mildly oxidized cytosolic proteins are degraded by the proteasome system in a ubiquitin-dependent or -independent fashion or by a selective form of lysosomal degradation known as chaperone-mediated autophagy (CMA) (Dunlop et al., 2009; Cuervo, 2010; David et al., 2010; Tyedmers et al., 2010). For these proteins the low degree of oxidation still allows for the protein to be unfolded, which is a requirement for entry into the narrow catalytic chamber of the proteasome or the translocation channel that mediates substrate internalization into lysosomes via CMA (Dunlop et al., 2009; Cuervo, 2010; David et al., 2010). In contrast, proteins with extensive oxidative damage that cannot unfold are often organized into cytosolic insoluble protein aggregates that are no longer amenable for degradation through these systems. Two distinct aggregating compartments have been described in yeast: one for proteins that can disaggregate and be delivered to the proteasome for degradation, and a different compartment for those that are irreversibly aggregated (Kaganovich et al., 2008; Kopito, 2000). The generally

accepted mechanism for the degradation of these irreversibly aggregated protein inclusions is macroautophagy, a high-capability pathway that delivers cytosolic material to lysosomes inside double-membrane vesicles or autophagosomes (Cuervo et al., 2005). Cargo-recognition molecules such as p62 and NBR1 sequestrate aggregated proteins inside autophagosomes through a selective form of macroautophagy known as aggrephagy (Lamark et al., 2009). For other types of protein aggregates, recruitment of cytosolic chaperones to the aggregate acts as a trigger for their degradation through a macroautophagy variant known as chaperone-assisted selective autophagy (CASA) (Arndt et al., 2010). Late endosomes and lysosomes are the final destination of these aggregate materials after fusion with the autophagosome carriers (Cuervo et al., 2005). In addition extracellular aggregates organized as amyloid-like structures can also reach late endosomes and lysosomes of tissue-resident macrophages and dendritic cells (DCs) after being phagocytosed (Chiti and Dobson, 2006; Alavez et al., 2011; Devitt and Marshall, 2011).

In endosomes/lysosomes most of the damaged biomolecules are degraded to their constitutive basic components by acidic hydrolases (Stern et al., 2006). However, the nature of the oxidized amino acid has an impact on protein turnover in that o- and m-tyrosines increase protein catabolism, whereas proteins with DOPA modifications are inefficiently degraded and tend to generate high-molecular weight (MW) SDS-stable aggregates (Dyer et al., 1993; Oliver et al., 1987; Requena et al., 2001; Dalle-Donne et al., 2003; Isom et al., 2004; Dunlop et al., 2008, 2009; Madian and Regnier, 2010). These aggregates can then enlarge by entanglement with nonoxidatively damaged proteins, furthering cellular toxicity (Squier, 2001; Cowan et al., 2003; Terman, 2006).

The increased level of free radicals reported in aging cells includes cells of the immune system (de la Fuente et al., 2004; Larbi et al., 2004; Nomellini et al., 2008). Additionally, a decreased level/functionality of the enzymes involved in clearance of free radicals, including catalase and glutathione peroxidase, has also been reported in aged immune cells (Fujimoto et al., 2010). The oxidative posttranslational modifications occurring on several proteins have been associated with compromised phagocytosis, proteasomal activity, and TLR signaling (Ponnappan et al., 2007; Shaw et al., 2010; West et al., 2010). In aging T cells, oxidative stress has been linked to increased protein carbonylation and glutathionylation of several cytoskeletal, ribosomal, and enzymatic proteins, with overall decreased cell functionality (Preynat-Seauve et al., 2003; Larbi et al., 2007; Hung et al., 2010). Finally, oxidative damage to adaptors of the TCR signal transduction machinery has been associated with a decrease in the intensity and length of the activation signal following TCR engagement in aging T cells (Larbi et al., 2004, 2007).

An aspect of immunosenescence that has not been investigated is whether age-related oxidative stress also compromises the biological functions of DCs and in particular, the ability of DCs to process and present MHC class II-restricted antigens. As such, the goal of our analysis was 2-fold: first, to qualitatively and quantitatively analyze the presence of oxidatively damaged proteins in DCs from aging mice; and second, to investigate whether oxidative stress interferes with MHC class II-restricted presentation and the overall ability to mount an effective immune response.

RESULTS

Accumulation of Oxidatively Damaged Proteins in DCs from Aging Lymphatic Organs

A hallmark of aging is an imbalance between production and clearance of ROS, as well as the intra- and extracellular accumulation of their by-products, namely oxidized proteins, advanced glycation end (AGE) products, and lipid oxidation products (Oliver et al., 1987; Dyer et al., 1993; Barja and Herrero, 2000; Dufour et al., 2000; Dalle-Donne et al., 2003; Starkov et al., 2004; Lin and Beal, 2006; Terman, 2006; Halliwell, 2009; Chandel, 2010; Hamanaka and Chandel, 2010; Madian and Regnier, 2010; Wellen and Thompson, 2010; Cannizzo et al., 2011). Oxidatively damaged biomolecules have been shown to compromise cellular functions in several dividing and nondividing cells (Preynat-Seauve et al., 2003; de la Fuente et al., 2004; Larbi et al., 2004, 2007; Ponnappan et al., 2007; Nomellini et al., 2008; Fujimoto et al., 2010; Hung et al., 2010; West et al., 2010). However, whether by-products of oxidative stress accumulate in primary and secondary lymphatic organs and whether their possible accumulation affects the ability of DCs to mount an adaptive immune response are currently unknown.

To address this question, we isolated $CD34^+$ bone marrow precursors: the progenitor cells that give rise to several of the hematopoietic cell lineages including DCs. $CD11c^+$ conventional DCs were also isolated from different lymphatic organs, including bone marrow, spleen, and peripheral lymph nodes, or cultured from bone marrow precursors derived from 3-, 12-, and 22-month-old mice. The presence of oxidative damage in $CD34^+$ cells would indicate that DC precursors are already compromised in their cellular proteome and likely give rise to functionally less efficient DCs.

To test for the presence of oxidatively damaged proteins, total cell lysates were incubated with 2,4-dinitrophenylhydrazine (DNPH), which selectively binds to carbonyl groups (ketone or aldehyde) that are added to amino acids side chains as an oxidative irreversible modification. Lysates were run on a 4%–15% gradient SDS-PAGE and the blotted membrane developed using an anti-DNPH mAb. Oxidatively carbonylated proteins could be detected in cells derived from all age mice groups, albeit at much higher levels in aging mice (Figures 1A–1F and S1). Interestingly, increased age-related protein carbonylation was observed in $CD34^+$-isolated bone marrow cells and conventional DCs cultured from bone marrow precursors, indicating that in aging mice even precursor cells or newly differentiated DCs accumulate biomarkers of oxidative stress (Figures 1A and 1B). Besides carbonylation, an increased amount of lipoxidation was also observed in old mice, as detected by probing for malondialdehyde, a highly reactive compound derived from the oxidative degradation of polyunsaturated lipids (Figure 1F).

In order to qualitatively analyze protein carbonylation, DNPH-bound proteins were immunoprecipitated from splenic $CD11c^+$ DCs purified from 22-month-old mice, and MS/MS analysis was employed to map oxidized proteins (Figure 1G). As

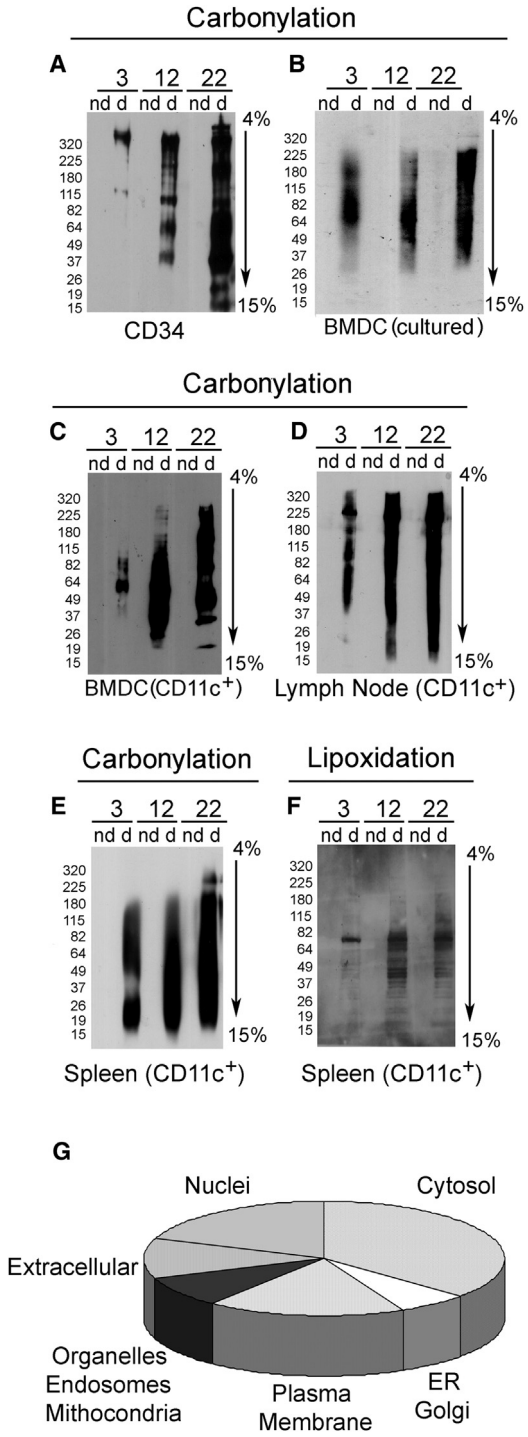

Figure 1. Detection of Oxidatively Modified Proteins in DCs Purified from Primary and Secondary Lymphatic Organs

(A–E) Western blot analysis of carbonylated proteins detected in (A) purified CD34$^+$ bone marrow precursors, (B) bone marrow dendritic cells (BMDC) cultured in GM-CSF for 7 days, and (C–E) conventional CD11c$^+$ DCs freshly purified from primary and secondary lymphatic organs from 3-, 12-, and 22-month-old mice is shown. Lanes marked as "d" report derivatized proteins and "nd" report nonderivatized proteins (specificity control). One representative experiment out of four is shown.

(F) Western blot analysis of lipoxidated proteins (probing for malondialdehyde) detected in conventional CD11c$^+$ freshly purified splenic DCs is presented. Loading controls are reported in Figure S1.

(G) Pie chart reporting the subcellular distribution of the oxidative proteome immunoprecipitate from conventional CD11c$^+$ splenic DCs purified from 22-month-old mice is demonstrated.

anticipated, oxidized proteins were derived from both intracellular and extracellular sources (Figure 1G; Tables S1 and S2). The former originated from oxidatively damaged organelles, nuclear proteins, cytosolic proteins, and the plasma membrane. The latter derived from phagocytosed oxidatively damaged extracellular matrix proteins (Figure 1G; Table S1). Ingenuity pathway analysis (IPA) was performed to determine the major networks associated with the oxidized proteome. Major pathways included enzymes involved in glycolysis, lipolysis, DNA repair, mitochondrial oxidative phosphorylation, extracellular tissue damage, and immunological functions. Taken together, the data indicate that the oxidative proteome could potentially interfere with several cellular biological functions.

Accumulation of Oxidatively Damaged Proteins in Endosomal Compartments of Aging DCs

We then mapped the modifications of amino acid side chains generated by ROS because it is known that individual oxidized species can target proteins for premature degradation or accumulation. For example hydroxyl or carbonyl modifications on some amino acids generate stable carbonylated proteins that are targeted for proteolysis, whereas hydroxyl attack on tyrosine or phenylalanine generates DOPA, which is a reactive species capable of further modifications including amplification of the oxidative damage to neighboring molecules (Dyer et al., 1993; Requena et al., 2001; Guptasarma et al., 1992; Sacksteder et al., 2006; David et al., 2010; Toda et al., 2010). Amino acids from the immunoprecipitated proteins fragmented by MS/MS (Table S1) were analyzed for oxidative posttranslational modifications. Only residues known to be primary targets of oxidation were analyzed (Table 1). Oxidative moieties comprised a large range of hydroxyl and carbonyl modifications (aldehyde and ketonic groups) and AGE products (Table 1). Additionally, 18% of phenylalanines and 7% of tyrosines were modified to generate DOPA, a moiety known to induce protein aggregation and accumulation into misfolded, protease-resistant high-MW aggregates (Table 1). Tryptophan, methionine, and cysteine have also been reported to undergo oxidation during aging (Requena et al., 2001; Squier, 2001; Guptasarma et al., 1992; Dalle-Donne et al., 2003; Madian and Regnier, 2010; Toda et al., 2010), and our results for DCs derived from 22-month-old mice were consistent with these finding. Tryptophan was found to be oxidized to hydroxykynurenin (4%), oxolactone (16.5%), and kynurenin (13.5%), in addition to the hydroxyl and dihydroxy species (40%), showing that more than 70% of this amino acid was in the oxidized state. Methionine was oxidized to met-sulphoxide (30.1%) and sulfones (20.1%). Cysteine underwent oxidation to cysteine sulfinic acid (dioxidation) (34.7%) and cysteic acid (trioxidation) (31.5%). Thus, more than 60% of tryptophan, methionine, and cysteine was shown to be in the oxidized forms. Other oxidations on arginine, lysine, proline, and histidine were

Table 1. Quantification of the Number of Amino Acids with Posttranslational Oxidative Modifications

Amino Acid	Chemical Modifications	%
Serine	Unmodified	91.5
	Glucuronyl	8.5
Cysteine	Unmodified	32.8
	Dioxidation (cysteine sulfinic acid)	35.7
	Trioxidation (cysteic acid)	31.5
Lysine	Unmodified	53.6
	Oxidation (hydroxy-Lys)	26.4
	Dioxidation (dihydroxy-Lys)	17.0
	Glucosylgalactosyl	3.0
Arginine	Unmodified	58.5
	Oxidation	21.6
	Dioxidation (hydroperoxide)	11.8
	3-deoxyglucosone (AGE derivative)	8.1
Tryptophan	Unmodified	30.0
	Oxidation (hydroxy-Trp/oxindolylalanine)	22.5
	Dioxidation (dioxindolylalanine/ N-formylkynurenine)	13.5
	Kynurenin	13.5
	Oxolactone	16.5
	Hydroxykynurenin	4.0
Methionine	Unmodified	49.8
	Oxidation (Met-sulphoxide)	30.1
	Dioxidation	20.1
Tyrosine	Unmodified	87.2
	Oxidation (meta- or ortho-hydroxy phenylalanine)	5.8
	Dioxidation (3,4 dihydroxy-phenylalanine [DOPA])	7.0
Phenylalanine	Unmodified	64.8
	Oxidation (meta- or ortho-Tyrosine)	17.2
	Dioxidation (DOPA)	18.0
Proline	Unmodified	38.2
	Oxidation (hydroxy-proline)	37.6
	Dioxidation (dihydroxy-proline)	24.2
Aspartate	Unmodified	78.5
	Oxidation (hydroxy aspartic acid)	21.5
Histidine	Unmodified	85.0
	Oxidation (2-oxo-histidine)	15.0
Asparagine	Unmodified	81.9
	Oxidation	18.1

Calculated from proteins listed in Table S1.

found to be between 50% and 60%. Histidine and asparagine displayed a lower level of oxidation (15%–20%) (Table 1). Altogether, the data support advanced oxidation of the DC proteome in 22-month-old mice.

Often, protein aggregates can form covalent bonds through Schiff base formation, which involves the interaction of a side-chain amine group with a carbonyl group. To determine the presence of high-MW protein aggregates, lysates of CD11c$^+$ splenic DCs from 3-, 12-, and 22-month-old mice were fractionated by gel filtration (Figure 2A). Before separation, proteins were incubated with DNPH to label the oxidized moieties. This procedure involves incubation in 6% SDS at pH 2, which can disentangle protein aggregates unless they have formed covalent bonds. Because our goal was to detect possible high-MW protein aggregates, the samples were run on an S-300 HR Sephacryl gel column. Dextran blue (MW of 2 × 10^6 kDa) was run as a high-MW marker (Figure 2A). Protein microaggregates could be detected around 1–3 million kDa (Figures 2A and 2B). Fractions collected before and around the dextran blue elution time were run on an SDS-PAGE and blotted for protein carbonylation. In all age groups oxidized proteins formed microaggregates in the high-MW range. However, in young mice the aggregates

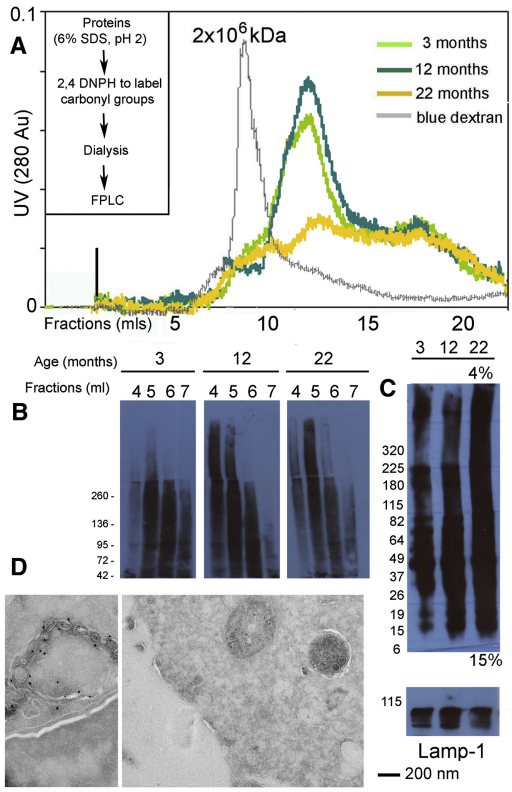

Figure 2. Accumulation of Microaggregates of Oxidatively Damaged Proteins in Splenic DCs Purified from Aging Mice

(A) FPLC separation of microaggregates of carbonylated proteins derived from CD11c$^+$ splenic DCs purified from 3-, 12-, and 22-month-old mice is illustrated. One preparation out of two is shown.

(B) Western blot analysis of the FPLC high-MW fractions to detect microaggregates of oxidized proteins is shown. Total cell lysates were prepared from CD11c$^+$ splenic DCs purified from the spleen of 3-, 12-, and 22-month-old mice. One preparation out of two is shown.

(C) Western blot analysis of carbonylated proteins detected in late endosomal compartments, gradient purified from splenic DCs of 3-, 12-, and 22-month-old mice is presented. LAMP1 immunoblot is shown as a loading control.

(D) Ultrastructural morphology of late endosomal multivesicular bodies (MVBs) from CD11c$^+$ splenic DCs purified from a 22-month-old mice is demonstrated. Immunogold labeling for MHC class II molecules (Ab clone AF120.6 is 5 nm gold, and Ab clone M5-114 is 10 nm gold) is illustrated.

were mostly transient and were solubilized by SDS, which did not occur in older mice (Figure 2B).

Most oxidatively damaged proteins present in the cytosol are processed through the proteasome or by CMA. However, heavily oxidized proteins that cannot unfold in order to enter the catalytic chamber of the proteasome or the translocation complex at the lysosomal membrane are transported to endosomal/lysosomal compartments by macroautophagy (Kopito, 2000; Kaganovich et al., 2008; Cuervo, 2010). Likewise, oxidatively damaged extracellular proteins, amyloid-like aggregates, and oxidatively damaged apoptotic cells are normally phagocytosed by tissue-resident macrophages and DCs (Chiti and Dobson, 2006; Alavez et al., 2011; Devitt and Marshall, 2011). Thus, we determined whether accumulation of oxidatively damaged proteins could be observed in endosomal compartments of DCs. To this end, splenic CD11c$^+$ DCs were generated from 3-, 12-, and 22-month-old mice (previously injected with B16-FLT3-L to expand the DC populations) and late endosomes separated over a 27:10 Percoll gradient. As described above, endosomal proteins were incubated with DNPH to label the oxidized moieties, before separation over a 4%–15% SDS-PAGE. Increased amounts of oxidatively damaged proteins could be observed in the endosomes of old mice compared with 3-month-old mice (Figure 2C).

Accumulations of lipofuscin aggregates are often observed with age in the endosomes of nondividing cells such as neurons, cardiomyocytes, and endothelial cells. To determine whether lipofuscin accumulation occurred in aging DCs, ultrastructural analysis of MHC II immunogold-labeled late endosomes was performed using two different antibodies (Abs) specific for I-A^b (Figure 2D). No lipofuscin deposits could be observed in these compartments in aging mice (Figure 2D). This is consistent with the notion that large aggregates only form in nondividing cells or cells with a very long life span, such as neurons, endothelial cells, and cardiomyocytes, where protein/lipid/carbohydrate aggregates form black lipofuscin inclusions, often of considerable size. DCs, even in old mice, have a turnover of 7–14 days; thus, accumulation of protein aggregates following oxidative stress does not result in the formation of visible lipofuscin inclusions (Figure 2D).

Altered Autophagy in Aging DCs

The accumulation of oxidatively damaged proteins in endosomal compartments of aging DCs prompted us to determine whether the sequestration and degradation capability of these compartments could be compromised. To this goal, we determined the rates of intracellular proteolysis in splenic DCs (CD11c$^+$) from 3-, 12-, and 22-month mice after labeling for 2 days with [^{3}H] leucine. During the 20 hr chase, cells were maintained in the presence or absence of a combination of ammonium chloride and leupeptin to block total lysosomal degradation (Figure 3A), or the PI3K inhibitor 3-methyladenine (3MA), widely used to inhibit macroautophagy (Figure 3B). These studies revealed a statistically significant decrease in total lysosomal degradation as well as basal 3MA-sensitive degradation in aging cells (Figures 3A and 3B).

To analyze further changes in macroautophagy activity with age in DCs, we directly measured the total amount and overall processing efficiency of the light-chain protein type 3 (LC3), a structural component of autophagosomes that undergoes degradation when these compartments fuse with lysosomes and late endosomes. Immunostaining for LC3 in CD11c$^+$ DCs purified from the spleen of 3-, 12-, and 22-month-old mice was used to visualize autophagosomes as LC3-positive fluorescent puncta by fluorescence microscopy with deconvolution. As shown in Figures 3C and 3D, the number of autophagosomes per cell was significantly increased in DCs in an age-dependent manner. An increase in autophagosome content can result from enhanced formation or decreased clearance of these compartments. To discriminate between these possibilities, we analyzed the LC3 flux by comparing levels of LC3-II, the autophagosome-associated form of the protein, in cells maintained in the presence or absence of inhibitors of lysosomal proteolysis. Immunoblot analysis of LC3-II in these experiments confirmed higher steady-state content of autophagosomes in old DCs (levels of LC3-II in untreated cells) (Figures 3E and 3F). In contrast, LC3-II flux was severely compromised in DCs from both 12- and 22-month-old mice, suggesting inefficient clearance of autophagosomes (Figure 3G). Consistent with the reduced rates of LC3 degradation, we also observed a moderate increase in total cellular levels of p62, a common autophagic cargo, although only at the most advanced ages (Figure S2). Levels of beclin 1, involved in initiation of autophagosome formation, and of Atg5, an essential component for the elongation of the autophagosome membrane, markedly increased with age in DCs (Figure S2). These results support the conclusion that induction and formation of autophagosomes are preserved until a late age in DCs and that one of the major steps altered in this process is the clearance of the autophagocytosed material.

Degradation of the autophagosome content can occur through fusion to both late endosomes and lysosomes. Under normal conditions most cells favor autophagosome fusion with secondary lysosomes because this compartment has a higher proteolytic capability; however, different reports support the conclusion that cells respond to compromised lysosome-autophagosome fusion by increasing fusion of autophagosomes with late endosomes to form a compartment described as amphisome. Analysis of the colocalization of cytosolic autophagic cargo (mitochondria) or structural autophagosome components (LC3) with the endocytic compartment (by assessing endocytosis of fluorescently labeled BSA) revealed a higher coincidence of these autophagosome and late endosomal markers in DCs of older animals (Figures 3H and 3I). These results indicate a higher macroautophagy-mediated transfer of cytosolic material, likely including oxidized microaggregated proteins, to the endosomal compartment of DCs with age and slower degradation of the cytosolic cargo in these compartments.

DCs from Aging Mice Have a Decreased In Vitro and In Vivo Ability to Process Exogenously Administered Antigen

In the next series of experiments, we set to determine whether cellular oxidative stress and accumulation of oxidatively damaged proteins in endosomal organelles compromised MHC II-restricted immune responses. To determine whether the reduced proteostasis would compromise adaptive immune

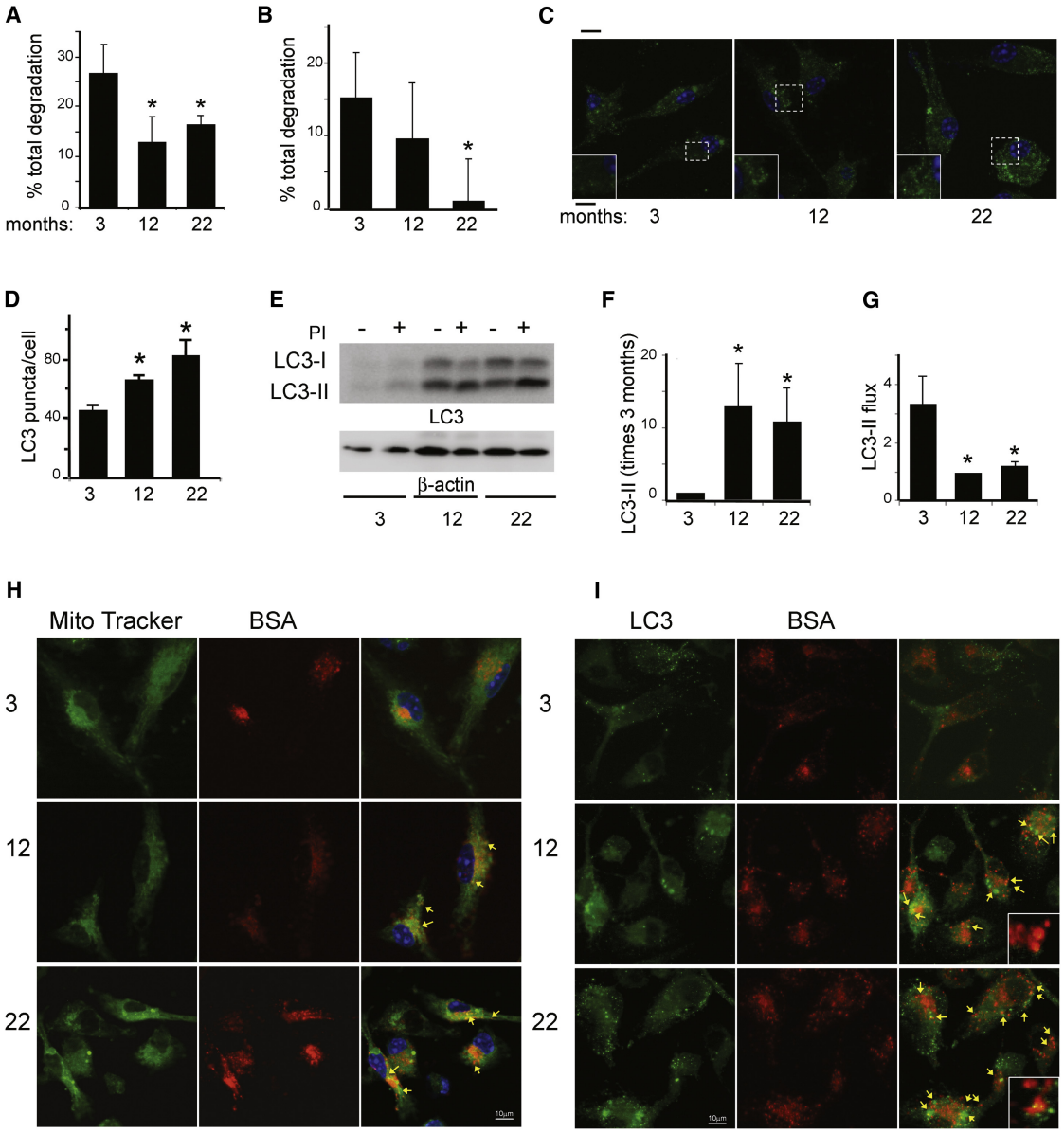

Figure 3. Decreased Endosomal/Lysosomal Degradation and Compromised Macroautophagy in DCs from Aging Mice

(A and B) CD11c$^+$ splenic DCs purified from 3-, 12-, and 22-month-old mice were labeled for 2 days with [^{3}H]leucine. During the chase, cells were maintained for 24 hr in the presence or absence of NH_4Cl/leupeptine (A) or 3MA (B) to block all lysosomal proteolysis or macroautophagy, respectively. Proteolysis rates for long-lived proteins after a 20 hr chase are shown. Values are the mean ± SD of three different experiments with triplicate wells. *$p < 0.05$.

(C) Immunofluorescence analysis of LC3 distribution in CD11c$^+$ splenic DCs from 3-, 12-, and 22-month-old mice is shown. Scale bar above the picture represents 10 mm; scale bar below the inset represents 2 mm.

(D) Quantification of the number of LC3-positive puncta per cell is presented. *$p < 0.05$.

(E–G) LC3 flux in CD11c$^+$ splenic DCs from 3-, 12-, and 22-month-old mice is demonstrated. Cells were incubated in the presence or absence of lysosomal protease inhibitors (PI) for 2 hr, collected and subjected to SDS-PAGE, and immunoblotted for LC3. (E) Representative immunoblot is illustrated. (F) Quantification of steady-state levels of LC3-II (content of autophagic vacuoles [AV]) and (G) LC3 flux (ratio of LC3-II in the presence and absence of protease inhibitors) is shown. *$p < 0.05$.

(H and I) Immunofluorescence of CD11c$^+$ splenic DCs from 3-, 12-, and 22-month-old mice (H) incubated with BSA-Alexa 647 and MitoTracker or (I) incubated with BSA-Alexa 647 and immunostained for LC3 is presented. Panels show individual channels and merged images. Arrows indicate points of convergence of the different fluorophores.

Insets in (C) and (I) are high magnification of cells depicted inside the dotted square. Scale bar above the picture is 10 μm; scale bar below the inset is 2 μm. Western blots for additional autophagy-relevant proteins are reported in Figure S2.

responses, 3-, 12-, and 22-month-old C57BL/6 (I-A^b) mice were injected in the flanks with 50 μg of Eα-RFP protein. Six or 12 hr later, $CD11c^+$ DCs were purified from the inguinal-draining lymph nodes of each age group, and the amount of MHC class II (I-A^b) was loaded with the Eα 52-68 peptide analyzed by surface staining using the conformational Ab Y-Ae (Figure 4A). A significant decrease in the amount of MHC class II/Eα 52-68-loaded complexes was observed on the plasma membrane of DCs from 22- and 12-month-old mice as compared to 3-month-old mice, even when normalized to the total amount of MHC II molecules and MHC II-CLIP-loaded molecules (Figures 4A–4C).

To determine whether such differences in antigen presentation could also be observed following immunization, 3-, 12-, and 22-month-old C57BL/6 (I-A^b) mice were injected in the flanks with 100 μg of Eα-RFP protein in complete Freund's adjuvant (CFA). Two weeks later, $CD11c^+$ DCs were purified from the draining lymph nodes of each age group, and the amount of MHC class II (I-A^b) loaded with the Eα 52-68 peptide was analyzed by surface staining using the conformational Ab Y-Ae (Figure 4D). Again, a significant decrease in the number of DCs displaying MHC class II/Eα 52-68-loaded complexes was observed on DCs from 22- and 12-month-old mice as compared to 3-month-old mice (Figure 4D). As expected, a decreased surface amount of I-A^b loaded with the Eα-RFP 52-68 peptide resulted in a diminished T cell proliferative response (Figure 4E). Supporting an intrinsic defect in DC functions in old mice, decreased proliferation was also observed when DCs from 12- and 22-month-old mice were incubated with 3-month-old T cells (Figure S3). To further quantify the Eα-RFP 52-68 peptide loaded on I-Ab from nodal DCs, MHC II-eluted peptides were subjected to MS analysis (Figures 4F and 4G). Quantification of the eluted peptides was achieved by spiking the samples with known amounts of monoisotopic-labeled Eα-RFP 52-68 peptide (Figures 4F and 4G). The Eα-RFP 52-68 peptide envelope was easily detected in the mixture of peptides eluted from DCs purified from 3-month-old immunized mice (Figure 4F). MS/MS fragmentation confirmed the correct peptide sequence (Figure 4G), and a comparison with the standard peptide allowed us to quantify its amount, varying between 31 and 125 femtomoles in 2 separate experiments (Figure 4F). The amount of Eα-RFP 52-68 eluted from 22-month-old mice was below our level of detection.

To confirm these results in an additional antigen system, $CD11c^+$ splenic DCs were purified from 3-, 12-, and 22-month old CBA mice and pulsed for 1.5 hr with 40 μg of FITC-conjugated hen egg lysozyme (HEL) (HEL-FITC). Processing of phagocytosed HEL-FITC was monitored by FACS analysis, as disappearance of the FITC fluorescence and by appearance of positive staining for a conformational Ab (AW3.1), specific for I-A^k loaded with the HEL 48-61 peptide (Figure 5A). A lower amount of AW3.1 staining was observed in both 12- and 22-month-old mice at each time point as compared to 3-month-old mice (Figure 5A). On the other hand, a higher amount of unprocessed HEL-FITC was also observed in aging mice as compared to the 3 month old (Figure 5A).

Differences observed in the amount of Eα-RFP processing among the three age groups could be partially related to a differential rate of protein phagocytosis or endosomal trafficking. To control for this possibility, late endosomes were prepared from splenic DCs purified from 3-, 12-, and 22-month-old mice (previously injected with B16-FLT3-L to expand the DC populations) using a 10:27 Percoll gradient (Figure 5B). Purified organelles were then incubated with 5 μg of Eα-RFP, and the amount of overall processing was analyzed by silver staining at different time points (Figure 5C). In agreement with the antigen-processing and presentation assay on intact cells, an increased amount of nonprocessed protein following digestion was observed for organelles prepared from 12- and 22-month-old mice as compared with 3-month-old mice (Figures 5C and 5D). Mass spectrometry analysis performed on Eα-RFP peptides isolated from the organelles following protein digestion confirmed a decreased number of Eα-RFP-specific peptides in 12- and 22-, as compared to 3-month-old mice (Figure 5E). As expected from the equal surface amount of MHC class II among the three age groups, no differences in peptide loading were observed when the preprocessed peptide was added exogenously (Figure 5F). Taken together, the data indicate a compromised ability of antigen processing and presentation in DCs purified from aging mice.

In the next series of experiments, we asked whether decreased proteolytic activity could be the reason for decreased antigen processing observed in aging DCs. Total cell lysates from splenic $CD11c^+$ DCs purified from 3-, 12-, and 22-month-old C57BL6 mice were analyzed by western blotting for cathepsin L and S, and the interferon-γ-inducible lysosomal thiol reductase (GILT). No differences were observed in the total amount of enzymes among the three groups of mice as compared to the LAMP-1 loading control (Figure S4A). When endosomal proteolytic activity was quantified by flow cytometry, using a cysteine protease-specific probe (cathepsin B, L, and S) that only targets the active form of these enzymes, a similar amount of fluorescence was observed in 12- and 22-month-old DCs, as compared with the 3 month old (Figure S4B). These data indicate that the altered endosomal proteostasis observed in aging DCs is not related to impaired level or activity of endosomal cathepsins. Data are consistent with that previously observed in aging neurons, where engorgement of endosomal compartments with oxidatively damaged proteins induced a decrease in processing activity, despite an increase in the amount of active cathepsins (Takahashi et al., 2007).

In Vivo Decrease of Oxidative Stress Ameliorates MHC Class II-Restricted Immune Response to Immunizing Antigen

In the final series of experiments, we aimed to determine whether a cellular decrease in oxidative stress would increase the ability of DCs to process and present the immunodominant Eα-RFP 52-68 peptide following in vivo immunization with Eα-RFP. To this end, 22-month-old mice were immunized subcutaneously with 100 μg of Eα-RFP and treated with one intraperitoneal (i.p.) injection of the antioxidant pyrrolidine dithiocarbamate (PDTC) at the time of immunization as well as daily in the drinking water for 14 days. Two weeks following immunization, $CD11c^+$ DCs were purified from the draining lymph nodes and total proteins run on an SDS-PAGE. A decreased amount of high-MW microaggregates was observed in the treated samples

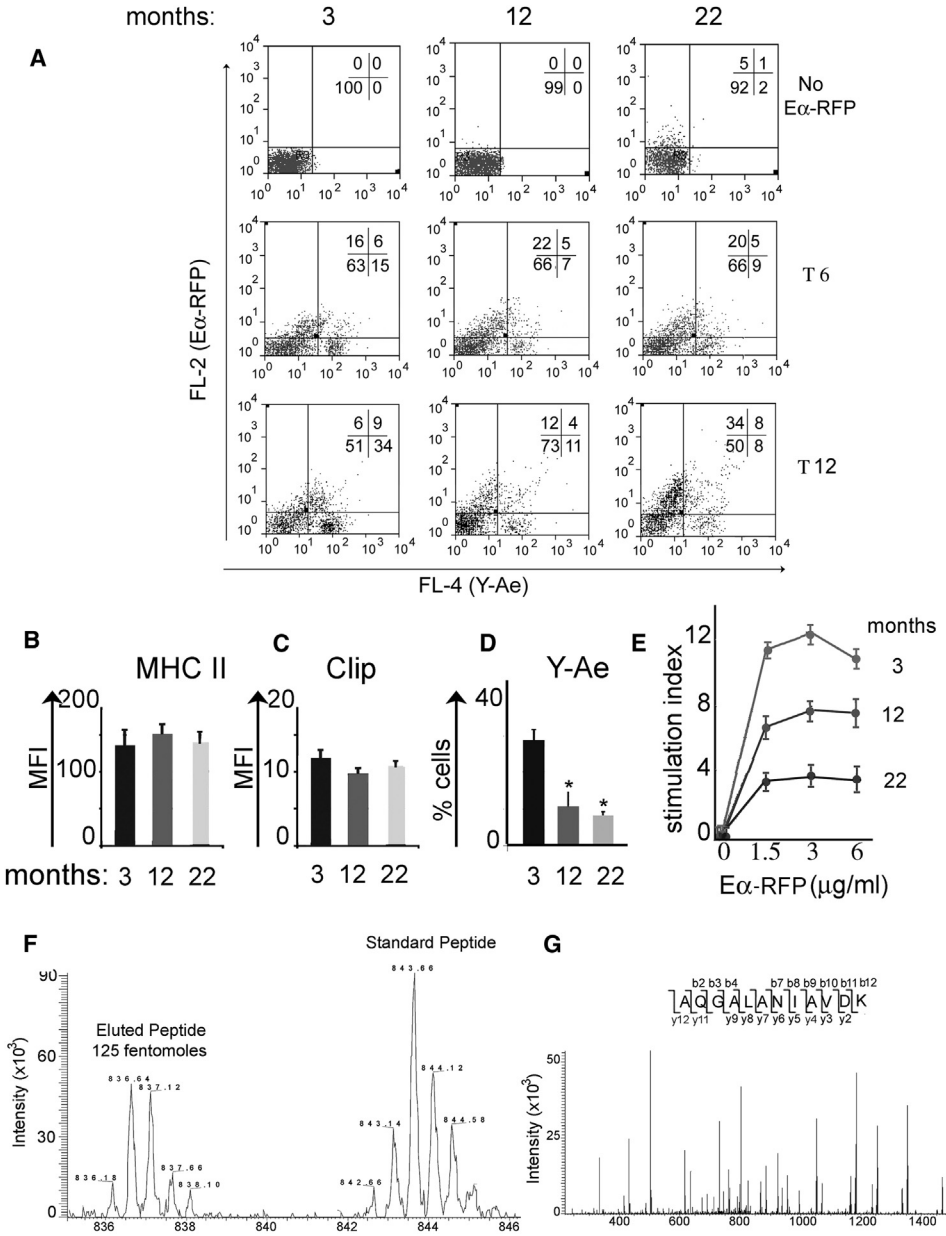

Figure 4. Decreased In Vivo Endosomal Processing and MHC Class II-Restricted Presentation in Conventional CD11c$^+$ DCs from Aging Mice

(A) FACS analysis of CD11c$^+$ splenic DCs, purified from 3-, 12-, and 22-month-old C57/Bl6 mice, following in vivo injection of Eα-RFP protein is demonstrated. Mice were injected with 50 μg/ml of Eα-RFP. CD11c$^+$ DCs were purified from the popliteal node and analyzed at different time points for RFP fluorescence, to quantify Eα-RFP processing, and Y-Ae staining to quantify I-Ab loading with the processed Eα 52-68 peptide. One representative experiment out of three is shown.

(B and C) Bar graph of the mean fluorescence index and SD of (B) total surface MHC class II protein (I-A^b) and (C) CLIP detected on the same CD11c$^+$ DC population is illustrated.

(D) Bar graph and SD of the percentage of CD11c$^+$ cells, which stained with the Y-Ae Ab (specific for I-A^b/Eα 52-68 complex), are shown. *$p < 0.05$. Lymph nodal CD11c$^+$ DCs were purified from 3-, 12-, and 22-month-old mice, immunized with 100 μg of Eα-RFP in CFA, 2 weeks earlier.

(E) T cell proliferative response from lymph nodes harvested from 3-, 12-, and 22-month old mice, previously immunized with 100 μg of Eα in CFA (one out of four experiments is shown) is presented.

(F) Quantitative MS scan of the immunodominant Eα 52-68 peptide eluted from nodal CD11c$^+$ DCs purified from 3-month-old mice previously immunized with 100 μg of Eα-RFP in CFA is demonstrated. Isotopically labeled Eα 52-68 peptide was spiked in the eluate for comparative quantification. One out of two quantifications is reported.

(G) MS/MS fragmentation of Eα 52-68 peptide eluted from nodal CD11c$^+$ DCs purified from 3-month-old mice previously immunized with 100 μg of Eα-RFP in CFA is illustrated.

Additional data on T cell proliferation are presented in Figure S3.

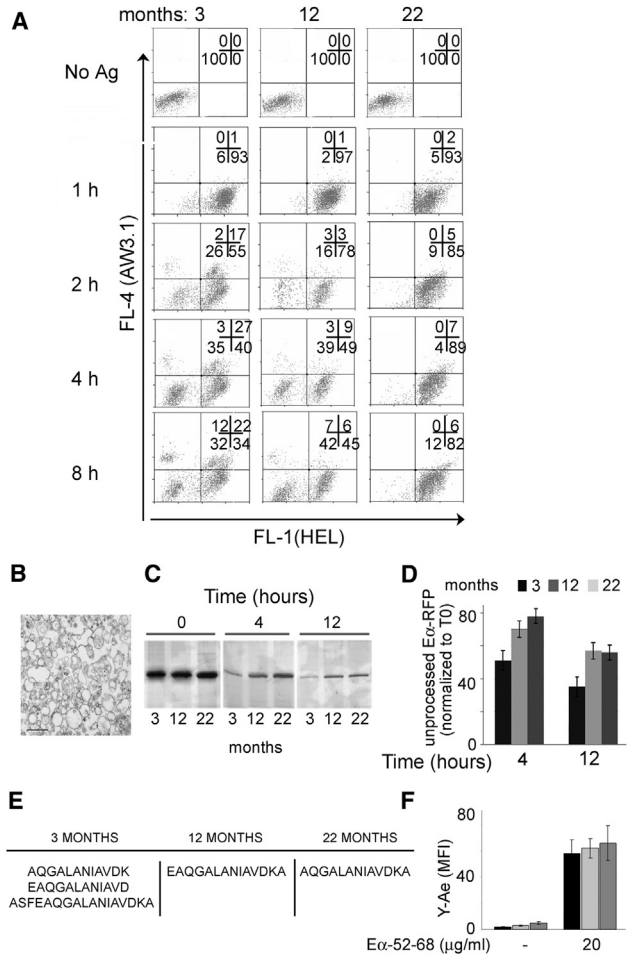

Figure 5. Decreased In Vitro Endosomal Processing and MHC Class II-Restricted Presentation in Conventional DCs from Aging Mice

(A) FACS analysis of CD11c$^+$ splenic DCs purified from 3-, 12-, and 22-month-old CBA mice, following phagocytosis of HEL-FITC protein, is shown. DCs were incubated with 20 μg/ml of HEL-FITC protein (time 0). Cells were then chased at different time points for FITC fluorescence to quantify HEL-FITC processing and AW3.1 staining to quantify I-A^k loading with the processed HEL 48-62 peptide. One representative experiment out of four is shown. No Ag, no antigen.

(B) Ultrastructural analysis of MVBs purified from CD11c$^+$ splenic DCs by a 10:27 Percoll gradient is presented. Scale bar represents 2 μm.

(C) Silver-stained SDS-PAGE of gradient-purified late endosomal compartments (3-, 12-, and 22-month-old mice) incubated for the indicated time points with 5 μg of recombinant Eα-RFP protein is demonstrated. Bands correspond to the amount of undigested Eα-RFP at the indicated time points.

(D) Bar graph and SD of the densitometric analysis of three independent endosomal-processing experiments as reported in (C) are illustrated. Data indicate the amount of Eα-RFP protein still unprocessed at different time points, calculated as percentage of total Eα-RFP (time 0).

(E) Peptide sequences, identified by MS/MS analysis, following endosomal Eα-RFP in vitro processing is shown. Data are collected from two sets of separate mass spectrometry analyses.

(F) Bar graph of the mean fluorescence index of Y-Ae surface staining of CD11c$^+$ splenic DCs harvested from 3-, 12-, and 22-month-old mice following incubation with or without Eα 52-68 peptide is presented. One experiment out of three is shown.

Additional data on endosomal cathepsin activity and western blot analysis of endosomal resident proteins are presented in Figure S4.

(Figure 6A). Similarly, a decreased amount of DNPH-detectable oxidized proteins could be observed following the in vivo treatment (Figure 6B). Importantly, the decrease in the overall amount of oxidative stress upregulated the amount of surface Y-Ae staining (specific for I-Ab-Eα-RFP 52-68) in 22-month-old mice (Figures 6C and 6D). Similarly, T cell proliferative responses were partially restored, as indicated by an increase in the stimulation index, in immunized PDTC-treated mice when compared to the untreated controls (Figure 6E).

Importantly, because it has been reported in different systems, whereas the antioxidant activity of PDTC restored biological functions in aging cells, it had the opposite effects on cells from young mice (Figure S5). This suggests that in aging cells the accumulated amounts of oxidized proteins are the major target for the redox activity of PDTC, whereas in young cells where there is a much lower amount of oxidized molecular targets, PDTC interferes with the cellular redox system that is pivotal to several biological activities (Figure S5).

DISCUSSION

Oxidative stress is a biological phenomenon that follows a biochemical imbalance between the formation and clearance/buffering of free radicals (Roberts and Sindhu, 2009; Haigis and Yankner, 2010). Oxidative stress is a common occurrence in cell biology; as such each organism is equipped with a variety of enzymes that specifically dispose of free radicals (Halliwell, 2009; Chandel, 2010; Hamanaka and Chandel, 2010; Wellen and Thompson, 2010; Cannizzo et al., 2011). However, in aging an increased production of ROS coupled with a decreased ability of the cell to dispose of them will often induce a chronic level of oxidative stress (Barja and Herrero, 2000; Dufour et al., 2000; Lin and Beal, 2006; Roberts and Sindhu, 2009; Haigis and Yankner, 2010; Cannizzo et al., 2011). The increased amount of highly reactive free radicals induces oxidative protein modifications, including direct amino acid oxidation with formation of carbonyl derivatives (aldehyde and ketonic groups on amino acid side chains), or indirect amino acid modifications by addition of peroxidated lipids or products from glycation and glycoxidation (Requena et al., 2001; Guptasarma et al., 1992; Sacksteder et al., 2006; Hung et al., 2010; Toda et al., 2010).

Oxidative modifications often result in protein fragmentation, dissociation, unfolding, exposure of hydrophobic residues and aggregation, and an overall loss of protein function (Dunlop et al., 2009; David et al., 2010; Tyedmers et al., 2010). When the oxidative damage is too extensive and irreversible, proteins are targeted for degradation. Two major factors determine the clearance of oxidized proteins: the overall amount of oxidized molecules, and their level of oxidation. Mildly oxidized cytosolic proteins are almost entirely degraded by the proteasome system and CMA because a low degree of oxidation still allows protein to unfold and enter the narrow proteasome catalytic chamber or the translocation lysosomal complex (Kopito, 2000; Kaganovich et al., 2008; Cuervo, 2010). In contrast extensively oxidized proteins aggregate to form an ''inclusion-like'' body, the aggresome, which is located in the cytosol at the microtubule-organizing center and which actively sequesters insoluble proteins (Kopito, 2000; Kaganovich et al., 2008). These aggregates can

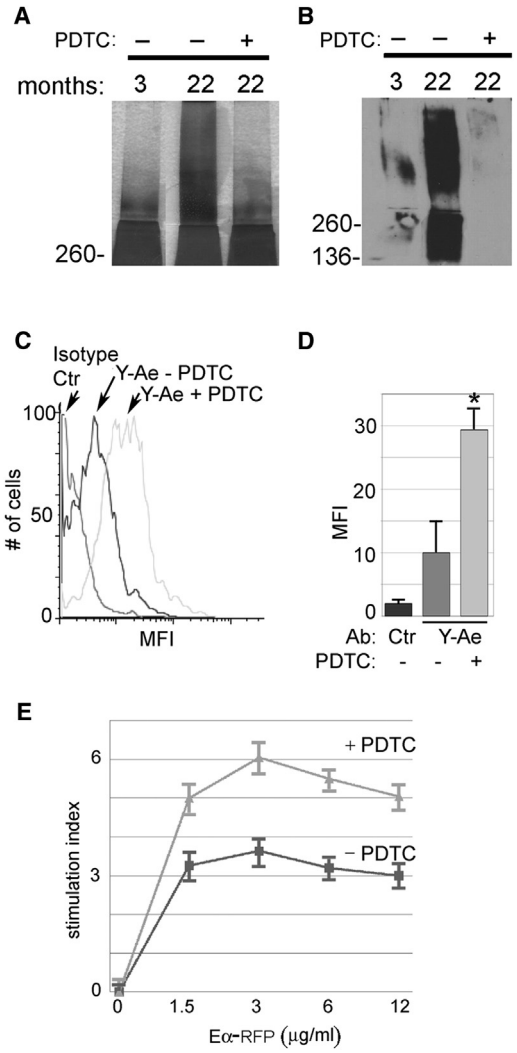

Figure 6. In Vivo Antioxidant Treatment Ameliorates MHC Class II-Restricted Immune Response to Immunizing Antigen

(A) Silver staining of protein microaggregates present in CD11c$^+$ DCs purified from the inguinal lymph nodes of 3- and 22-month-old mice untreated (–) or treated (+) with the antioxidant agent PDTC is demonstrated. One out of three experiments is reported.

(B) Western blot analysis of carbonylated proteins present in CD11c$^+$ DCs purified from the inguinal lymph nodes of 3- and 22-month-old mice untreated (–) or treated (+) with the antioxidant agent PDTC is illustrated. One out of three experiments is reported.

(C) Y-Ae surface staining of CD11c$^+$ splenic DCs harvested from 22-month-old mice untreated (–) or treated (+) with the antioxidant agent PDTC for 2 weeks is shown. After purification DCs were pulsed for 1 hr with 20 μg of Eα-RFP and chased overnight before staining with Y-Ae. Arrows indicate the histograms for each of the reported treatments. Ctr, control.

(D) Bar graph depicting the average and SD of Y-Ae staining collected as in (C) by four independent experiments is presented. *$p < 0.05$.

(E) T cell proliferative response from inguinal lymph nodes harvested from 22-month-old mice, previously immunized with 100 μg of Eα in CFA, untreated (–) or treated (+) with the antioxidant agent PDTC for 2 weeks following immunization is demonstrated. One of four experiments is shown.

PDTC treatment in young mice is reported in Figure S5.

be sequestered into the nascent autophagosome by a series of cargo-recognition proteins and cytosolic chaperones, and are then transported to the late endosomes and lysosomes by macroautophagy (Kopito, 2000; Kaganovich et al., 2008; Lamark et al., 2009). Additionally, extracellular-oxidized matrix and aggregates from apoptotic cells (apoptotic bodies) are delivered to endosomal compartments following phagocytosis by tissue-resident macrophages and DCs (Chiti and Dobson, 2006; Alavez et al., 2011; Devitt and Marshall, 2011).

In the endosomes, oxidatively damaged biomolecules are degraded to their constitutive amino acids by acidic endopeptidases. However, heavily oxidized proteins, crosslinked by disulphide bonds, aggregate into a mixture of protein lipid deposits that are often inaccessible to lysosomal hydrolases (Chiti and Dobson, 2006; Dunlop et al., 2009; David et al., 2010; Tyedmers et al., 2010). These aggregates can further enlarge over time by the addition of newly oxidized molecules, and induce endosomal destabilization and cytotoxic cell death (Dunlop et al., 2009).

Immunosenescence is characterized by a decreased ability of the immune system to respond to foreign antigens, as well as a decreased ability to maintain tolerance to self-antigens. This results in an increased susceptibility to infection and cancer, and reduced responses to vaccination (Linton and Dorshkind, 2004; Agrawal et al., 2007; Pawelec et al., 2010; Shaw et al., 2010). Innate immune responses such as phagocytosis, ROS production, and TLR function are generally compromised during immunosenescence (Bruunsgaard et al., 2001; de la Fuente et al., 2004; Nomellini et al., 2008; Agarwal and Busse, 2010; Fujimoto et al., 2010). Likewise, adaptive immune responses are hindered by a decrease in the variety of the B and T cell repertoires, as well as their ability to clonally expand following antigen stimulation (Fratelli et al., 2002; Larbi et al., 2007). Some controversy exists as to the capacity of DCs from aging mice to stimulate T and B cells. In mice there is a general agreement that splenic and nodal common DCs are impaired in their capacity to stimulate a proliferative response or to induce an antitumor immune response (Sharma et al., 2006). However, in aging subjects there is more disagreement. Some authors report a normal ability of DCs to stimulate T cells (Grewe, 2001), whereas others report that DCs purified from elderly subjects can activate memory, but not naive T cells (Agrawal et al., 2007). With regard to cytokine and chemokine production, several reports indicate a general dysregulation with aging, with a low-level chronic production of proinflammatory cytokines associated with decreased responsiveness to cytokine production following specific stimuli (Bruunsgaard et al., 2001; de la Fuente et al., 2004; Nomellini et al., 2008; Cannizzo et al., 2011).

In this report, using biochemical and biophysical techniques, we present evidence that in DCs purified from aging mice, the exogenous and endogenous antigen-processing and presentation pathways are impaired. Two major biochemical mechanisms can explain the impaired antigen-processing and presentation ability of DCs from aging mice: (1) the overall oxidative proteome could compromise the functionality of membrane organelles and cellular pathways associated with the antigen-processing and loading machinery; or (2) the overloading of endosomal compartments with oxidatively damaged proteins and protein/lipid microaggregates could interfere with efficient

endosomal proteostasis (Stadtman, 1992, 2004; Cloos and Christgau, 2004; Dunlop et al., 2008, 2009; Tyedmers et al., 2010). In favor of the first hypothesis are the data derived from the MS/MS mapping of the cellular oxidative proteome, which indicates that, indeed, proteins associated with many cellular pathways involved in protein trafficking, mitochondrial ATP generation, and overall cellular basic functions are oxidized. A question still lingering is the relationship between amino acid oxidation and protein loss of biological activity (Stadtman, 1992, 2004; Cloos and Christgau, 2004; Dunlop et al., 2008, 2009). In principle the number of oxidative moieties on a protein directly correlates with the loss of biological function because carbonylation is an irreversible posttranslational modification, and the higher the oxidation state, the higher is the likelihood that the protein would irreversibly unfold and lose its biological function. Additionally, oxidized proteins are targeted for degradation, and specific oxidations on specific amino acids can have a different impact on protein proteolysis directly increasing or decreasing the protein half-life. For example L-DOPA-modified proteins generate high-MW aggregates that are SDS stable and resistant to proteolysis, and upregulate the transcription and activity of endosomal cathepsins (S and L) (Rodgers et al., 2004). On the other hand, hydroxylation of the same amino acids results in increased protein catabolism (Dunlop et al., 2009). Currently, we do not know the level of oxidation, the half-life, and the residual biological activity for each of the proteins we identified by MS/MS as oxidatively modified and that are involved in antigen processing and presentation. However, we present evidence that a decrease in their level of oxidation increases the overall ability of DCs to process and present immunizing peptides (Rudensky et al., 1991; Murphy et al., 1992; Itano et al., 2003).

The second hypothesis is that overloading of endosomal compartments with oxidatively damaged proteins as well as microaggregates could interfere with efficient antigen processing. In favor of this hypothesis, we demonstrate that MHC class II-positive late endosomes do indeed accumulate protein microaggregates, which are greatly diminished by in vivo treatment with antioxidant. At the present time, we do not favor any of the two hypotheses, and we actually consider it more likely that oxidative stress compromises both the functionality of proteins involved in antigen processing and presentation as well as interferes with endosomal proteostasis following accumulation of insoluble protein aggregates, which hijack cathepsin activity as previously shown in other aging cells (Rodgers et al., 2004).

Finally, conventional DCs have a short half-life and are constantly replaced by bone marrow-derived circulating elements. Herein, we demonstrated that in aging mice, despite their short life span, these cells accumulate products of oxidative damage, likely because they are derived from an ''aging bone marrow'' that contains precursor elements already compromised by oxidative stress. This hypothesis is supported by our results indicating increased presence of carbonylated proteins in $CD34^{+}$ bone marrow cell precursors, freshly purified from 22-month-old mice. Additionally, the increased amount of aging-associated ROS in each parenchymal organ could further the cellular damage of newly generated DCs. The short life span of DCs could also be the main reason of why the in vivo therapy with antioxidant scavengers proved to be so effective. In fact by treating the mice for 2 weeks with an antioxidant, we could reduce the amount of carbonylated proteins in the newly generated DCs and increase the cells' overall biological performance, something that could not be attainable in cells with a much longer life span.

Taken together, our analysis reports in a qualitative and quantitative manner the presence of increased protein carbonylation, glycation, and lipoxidation in DCs purified from lymphatic organs of aging mice. Microaggregates of oxidatively damaged proteins were found in endosomal compartments likely transported by autophagic pathways (Cuervo, 2010; Sahu et al., 2011). The data support the conclusion that age-related oxidative stress interferes with the ability to mount an MHC class II-restricted immune response and that this function can be partially restored following in vivo antioxidant therapy.

EXPERIMENTAL PROCEDURES

Mice and Mice Treatments

C57BL/6J and CBA mice (3, 12, and 22 months old) were purchased from Harlam as part of the age-controlled NIH mouse colony program. All animal procedures were carried out according to a protocol approved by the Institutional Animal Care of Albert Einstein College of Medicine. In some experiments mice were injected in the flanks with 50 μg of Eα-RFP protein, and inguinal lymph nodes were collected after 6 or 24 hr. In other experiments mice were immunized in the flanks and nape of the neck with 100 μg of Eα-RFP protein in CFA, and axillary and inguinal lymph nodes were harvested 2 weeks later. In other experiments following immunization mice received a single i.p. injection of ammonium PDTC (Sigma-Aldrich, St. Louis) (50 mg/kg), followed by oral PDTC treatment (5 mg/ml in drinking water) for 2 weeks. In some experiments (Figures 4F and 4G), splenic DCs were expanded in vivo to obtain a sufficient number of cells for MHC II peptide elution. Mice were injected subcutaneously with the B16-FLT3L line. Spleens were collected after 2 weeks.

Preparation of Eα-RFP and HEL-FITC

Eα-RFP (Itano et al., 2003) protein expression plasmid was generously provided by Denzin Lisa (Memorial Sloan Kettering, New York). Protein production was induced with 1 mM IPTG for 48 hr, and the Eα-RFP protein was purified from the bacterial lysate using a Ni^{2+}-charged His-Bind resin column (Novagen; EMD Chemicals, Gibson, NJ, USA) followed by FPLC purification. Protein expression and purity were assessed by SDS-PAGE followed by silver staining. Five milligrams of HEL (>98% purity; Sigma-Aldrich) was incubated with 200 μl of FITC solution (stock 10 mg/ml in DMSO) in sodium bicarbonate buffer (pH >8.0–9.0) at room temperature for 1 hr. The free dye was removed from the labeled protein by dialysis. The total amount of labeled protein was calculated with the following formula: (moles/liter = [A280 − (A494 × 0.3)] × dilution factor)/38,940, where 38,940 is the molar extinction coefficient (moles − 1 cm − 1) for the dye. On average five to ten FITC molecules/protein were incorporated.

T Cell Proliferation

Inguinal and axillary lymph nodes were harvested 2 weeks after immunization, and 6×10^5 cells were seeded in a 96-well plate with or without titrated amounts of the immunizing antigen for 72 hr. Thymidine (1 μCu) was added 18 hr before cell harvesting. Cells were harvested on a Tomtec harvester (Model 94-3-468), and incorporated thymidine was counted on a liquid scintillation counter (1450 MicroBeta Wallac TriLux).

Flow Cytometry

Nodal or splenic purified DCs were incubated for 30 min on ice with saturating amounts of anti-Y-Ae Alexa 647 (gift from Lisa Denzin, Memorial Sloan Kettering), AW3.1-FITC (gift from Emil Unanue, Washington University), rat anti-mouse IA/IE (clone M5114; PharMingen), or $I\text{-}A^{b}$-CLIP (gift from Paul Roche,

NIH) in staining buffer (PBS, 0.1% BSA, 0.01% NaN_3). Following washing in staining buffer, samples were analyzed with the FACScan flow cytometer (Becton Dickinson, Franklin Lakes, NJ, USA).

Antigen-Processing Assay

$CD11c^+$ DCs, purified by magnetic bead immunoselection (Miltenyi Biotec), were pulsed with 20 μg of Eα-RFP or HEL-FITC for 1 hr. Cells were then washed in PBS and chased for different time points. After collection DCs were analyzed by FACS to detect processing of Eα-RFP or HEL-FITC proteins as well as MHC class II-loading $I\text{-}A^b$/Eα 52-68 and $I\text{-}A^k$/HEL 48-61.

Western Blot Analysis

A list of Abs and procedures are reported in Extended Experimental Procedures.

Fluorescence Microscopy

$CD11c^+$ DCs were grown on coverslips, fixed for 10 min in either ice-cold methanol or 4% formaldehyde in PBS, blocked and permeabilized (1% BSA, 2% newborn calf serum, 0.01% Triton X-100), and then incubated with the primary LC3 and corresponding Alexa 488 or cyanine 5-conjugated secondary Abs as described previously by Kaushik et al. (2006). After immunostaining, cells were rinsed with PBS and mounted for microscopy using Fluoromount-G (Southern Biotech). Images were collected using an Axiovert 200 fluorescence microscope (Carl Zeiss) equipped with a ×63 objective, 1.4 numerical aperture, and ApoTome. Quantification was performed on images with maximum projection of all z stack sections using ImageJ (NIH) after thresholding. Particle number was quantified with the "analyze particles" function in thresholded images with size (pixel $\geq$2) settings from 0.1 to 10 and circularity 0–1. Where indicated, cells were incubated with MitoTracker (Molecular Probes) for 15 min, or BSA-Alexa 647 for 30 min, rinsed with PBS, and processed for immunofluorescence as detailed above.

Endosomal Subcellular Fractionation and Eα-RFP In Vitro Processing

Splenic $CD11c^+$ DCs purified from 3-, 12-, and 22-month-old mice, previously injected with the B16-FLT3L line, were collected, homogenized, and then fractionated on consecutive Percoll gradient (27% and 10%) as previously described by Sahu et al. (2011). Ten micrograms of late endosomes, from each age group, was incubated with 5 μg of Eα-RFP in 120 mM Na-acetate (pH 5) at 37°C. After 30 min, samples were collected and run on a 12% SDS-PAGE. Eα-RFP digestion was monitored by silver staining (Pierce Silver Staining Kit; Thermo Scientific).

LTQ-Tandem MS/MS Sequencing

Three sets of experimental samples were analyzed by MS/MS: (1) DNPH immunoprecipitate of oxidized proteins (Figures 1G, 1H, and 2A; Tables S1 and S2); (2) samples derived from Eα-RFP processing by purified endosomal compartments (Figure 5E); and (3) samples eluted from surface MHC II proteins from DCs of 3-, 12-, and 22-month-old mice immunized with Eα-RFP (Figures 4F and 4G). Following incubation at 37°C with purified endosomal compartments, the reaction was stopped with 0.5% TFA. Processed and MHC class II-eluted peptides were retrieved by filtration through 10 kDa Millipore devices and subjected to MS/MS peptide sequencing. Purified splenic DCs from 3-, 12-, and 22-month-old mice were lysed and subjected to DNPH immunoprecipitation of carbonyl-modified proteins. The eluted samples were run on a 10% SDS-PAGE. The gel was silver stained, and the proteins were excised from both the stacking and the resolving part of the gel. LTQ-MS/MS sequencing was performed using a Nanospray LC-MS/MS on a LTQ linear ion trap mass spectrometer (LTQ; Thermo Scientific, San Jose, CA, USA) interfaced with a TriVersa NanoMate nanoelectrospry ion source (Advion BioSciences, Ithaca, NY, USA).

Statistical Analysis

Numerical results are reported as mean + SE. Data are derived from a minimum of three independent experiments unless stated otherwise. Statistical significance of the difference between experimental groups, in instances of multiple means comparisons, was determined using one-way ANOVA, followed by the Bonferroni post hoc test. Differences were considered significant for $p < 0.05$.

SUPPLEMENTAL INFORMATION

Supplemental Information includes Extended Experimental Procedures, five figures, and two tables and can be found with this article online at http://dx.doi.org/10.1016/j.celrep.2012.06.005.

LICENSING INFORMATION

ACKNOWLEDGMENTS

This work was supported by the National Institutes of Health Grants AI48833 to L.S. and AG031782 and DK041918 to A.M.C., F.M., and L.S., and a National Institute on Aging Training Grant to S.K. L.N.A. was supported by the NIH Fogarty Geographic Infectious Diseases Training Grant D43TW007129.

Received: December 8, 2011
Revised: April 23, 2012
Accepted: June 6, 2012
Published online: July 12, 2012

REFERENCES

Agarwal, S., and Busse, P.J. (2010). Innate and adaptive immunosenescence. Ann. Allergy Asthma Immunol. *104*, 183–190.

Agrawal, A., Agrawal, S., and Gupta, S. (2007). Dendritic cells in human aging. Exp. Gerontol. *42*, 421–426.

Alavez, S., Vantipalli, M.C., Zucker, D.J., Klang, I.M., and Lithgow, G.J. (2011). Amyloid-binding compounds maintain protein homeostasis during ageing and extend lifespan. Nature *472*, 226–229.

Alexeyev, M.F. (2009). Is there more to aging than mitochondrial DNA and reactive oxygen species? FEBS J. *276*, 5768–5787.

Arndt, V., Dick, N., Tawo, R., Dreiseidler, M., Wenzel, D., Hesse, M., Fürst, D.O., Saftig, P., Saint, R., Fleischmann, B.K., et al. (2010). Chaperone-assisted selective autophagy is essential for muscle maintenance. Curr. Biol. *20*, 143–148.

Barja, G., and Herrero, A. (2000). Oxidative damage to mitochondrial DNA is inversely related to maximum life span in the heart and brain of mammals. FASEB J. *14*, 312–318.

Broadley, S.A., and Hartl, F.U. (2008). Mitochondrial stress signaling: a pathway unfolds. Trends Cell Biol. *18*, 1–4.

Bruunsgaard, H., Pedersen, M., and Pedersen, B.K. (2001). Aging and proinflammatory cytokines. Curr. Opin. Hematol. *8*, 131–136.

Cannizzo, E.S., Clement, C.C., Sahu, R., Follo, C., and Santambrogio, L. (2011). Oxidative stress, inflamm-aging and immunosenescence. J. Proteomics *74*, 2313–2323.

Cathcart, M.K. (2004). Regulation of superoxide anion production by NADPH oxidase in monocytes/macrophages: contributions to atherosclerosis. Arterioscler. Thromb. Vasc. Biol. *24*, 23–28.

Chandel, N.S. (2010). Mitochondrial regulation of oxygen sensing. Adv. Exp. Med. Biol. *661*, 339–354.

Chiti, F., and Dobson, C.M. (2006). Protein misfolding, functional amyloid, and human disease. Annu. Rev. Biochem. *75*, 333–366.

Cloos, P.A., and Christgau, S. (2004). Post-translational modifications of proteins: implications for aging, antigen recognition, and autoimmunity. Biogerontology *5*, 139–158.

Cowan, K.J., Diamond, M.I., and Welch, W.J. (2003). Polyglutamine protein aggregation and toxicity are linked to the cellular stress response. Hum. Mol. Genet. *12*, 1377–1391.

Cuervo, A.M. (2010). Chaperone-mediated autophagy: selectivity pays off. Trends Endocrinol. Metab. *21*, 142–150.

Cuervo, A.M., Bergamini, E., Brunk, U.T., Dröge, W., Ffrench, M., and Terman, A. (2005). Autophagy and aging: the importance of maintaining "clean" cells. Autophagy *1*, 131–140.

Dale, D.C., Boxer, L., and Liles, W.C. (2008). The phagocytes: neutrophils and monocytes. Blood *112*, 935–945.

Dalle-Donne, I., Rossi, R., Giustarini, D., Milzani, A., and Colombo, R. (2003). Protein carbonyl groups as biomarkers of oxidative stress. Clin. Chim. Acta *329*, 23–38.

David, D.C., Ollikainen, N., Trinidad, J.C., Cary, M.P., Burlingame, A.L., and Kenyon, C. (2010). Widespread protein aggregation as an inherent part of aging in *C. elegans*. PLoS Biol. *8*, e1000450.

de la Fuente, M., Hernanz, A., Guayerbas, N., Alvarez, P., and Alvarado, C. (2004). Changes with age in peritoneal macrophage functions. Implication of leukocytes in the oxidative stress of senescence. Cell. Mol. Biol. (Noisy-le-grand), 50 Online Pub, OL683–OL690.

Devitt, A., and Marshall, L.J. (2011). The innate immune system and the clearance of apoptotic cells. J. Leukoc. Biol. *90*, 447–457.

Dufour, E., Boulay, J., Rincheval, V., and Sainsard-Chanet, A. (2000). A causal link between respiration and senescence in *Podospora anserina*. Proc. Natl. Acad. Sci. USA *97*, 4138–4143.

Dunlop, R.A., Dean, R.T., and Rodgers, K.J. (2008). The impact of specific oxidized amino acids on protein turnover in J774 cells. Biochem. J. *410*, 131–140.

Dunlop, R.A., Brunk, U.T., and Rodgers, K.J. (2009). Oxidized proteins: mechanisms of removal and consequences of accumulation. IUBMB Life *61*, 522–527.

Durieux, J., Wolff, S., and Dillin, A. (2011). The cell-non-autonomous nature of electron transport chain-mediated longevity. Cell *144*, 79–91.

Dyer, D.G., Dunn, J.A., Thorpe, S.R., Bailie, K.E., Lyons, T.J., McCance, D.R., and Baynes, J.W. (1993). Accumulation of Maillard reaction products in skin collagen in diabetes and aging. J. Clin. Invest. *91*, 2463–2469.

Fratelli, M., Demol, H., Puype, M., Casagrande, S., Eberini, I., Salmona, M., Bonetto, V., Mengozzi, M., Duffieux, F., Miclet, E., et al. (2002). Identification by redox proteomics of glutathionylated proteins in oxidatively stressed human T lymphocytes. Proc. Natl. Acad. Sci. USA *99*, 3505–3510.

Fujimoto, H., Kobayashi, H., and Ohno, M. (2010). Age-induce reduction in mitochondrial manganese superoxide dismutase activity and tolerance of macrophages against apoptosis induced by oxidized low density lipoprotein. Circ. J. *74*, 353–360.

Grewe, M. (2001). Chronological ageing and photoageing of dendritic cells. Clin. Exp. Dermatol. *26*, 608–612.

Guptasarma, P., Balasubramanian, D., Matsugo, S., and Saito, I. (1992). Hydroxyl radical mediated damage to proteins, with special reference to the crystallins. Biochemistry *31*, 4296–4303.

Haigis, M.C., and Yankner, B.A. (2010). The aging stress response. Mol. Cell *40*, 333–344.

Halliwell, B. (2009). The wanderings of a free radical. Free Radic. Biol. Med. *46*, 531–542.

Hamanaka, R.B., and Chandel, N.S. (2010). Mitochondrial reactive oxygen species regulate cellular signaling and dictate biological outcomes. Trends Biochem. Sci. *35*, 505–513.

Hung, L.F., Huang, K.Y., Yang, D.H., Chang, D.M., Lai, J.H., and Ho, L.J. (2010). Advanced glycation end products induce T cell apoptosis: involvement of oxidative stress, caspase and the mitochondrial pathway. Mech. Ageing Dev. *131*, 682–691.

Isom, A.L., Barnes, S., Wilson, L., Kirk, M., Coward, L., and Darley-Usmar, V. (2004). Modification of Cytochrome c by 4-hydroxy- 2-nonenal: evidence for histidine, lysine, and arginine-aldehyde adducts. J. Am. Soc. Mass Spectrom. *15*, 1136–1147.

Itano, A.A., McSorley, S.J., Reinhardt, R.L., Ehst, B.D., Ingulli, E., Rudensky, A.Y., and Jenkins, M.K. (2003). Distinct dendritic cell populations sequentially present antigen to CD4 T cells and stimulate different aspects of cell-mediated immunity. Immunity *19*, 47–57.

Johnson, F., and Giulivi, C. (2005). Superoxide dismutases and their impact upon human health. Mol. Aspects Med. *26*, 340–352.

Kaganovich, D., Kopito, R., and Frydman, J. (2008). Misfolded proteins partition between two distinct quality control compartments. Nature *454*, 1088–1095.

Kaushik, S., Massey, A.C., and Cuervo, A.M. (2006). Lysosome membrane lipid microdomains: novel regulators of chaperone-mediated autophagy. EMBO J. *25*, 3921–3933.

Klebanoff, S.J. (2005). Myeloperoxidase: friend and foe. J. Leukoc. Biol. *77*, 598–625.

Kopito, R.R. (2000). Aggresomes, inclusion bodies and protein aggregation. Trends Cell Biol. *10*, 524–530.

Lamark, T., Kirkin, V., Dikic, I., and Johansen, T. (2009). NBR1 and p62 as cargo receptors for selective autophagy of ubiquitinated targets. Cell Cycle *8*, 1986–1990.

Larbi, A., Dupuis, G., Douziech, N., Khalil, A., and Fülöp, T., Jr. (2004). Low-grade inflammation with aging has consequences for T-lymphocyte signaling. Ann. N Y Acad. Sci. *1030*, 125–133.

Larbi, A., Kempf, J., and Pawelec, G. (2007). Oxidative stress modulation and T cell activation. Exp. Gerontol. *42*, 852–858.

Lin, M.T., and Beal, M.F. (2006). Mitochondrial dysfunction and oxidative stress in neurodegenerative diseases. Nature *443*, 787–795.

Linton, P.J., and Dorshkind, K. (2004). Age-related changes in lymphocyte development and function. Nat. Immunol. *5*, 133–139.

Madian, A.G., and Regnier, F.E. (2010). Proteomic identification of carbonylated proteins and their oxidation sites. J. Proteome Res. *9*, 3766–3780.

Murphy, D.B., Rath, S., Pizzo, E., Rudensky, A.Y., George, A., Larson, J.K., and Janeway, C.A., Jr. (1992). Monoclonal antibody detection of a major self peptide. MHC class II complex. J. Immunol. *148*, 3483–3491.

Nomellini, V., Gomez, C.R., and Kovacs, E.J. (2008). Aging and impairment of innate immunity. Contrib. Microbiol. *15*, 188–205.

Oliver, C.N., Ahn, B.W., Moerman, E.J., Goldstein, S., and Stadtman, E.R. (1987). Age-related changes in oxidized proteins. J. Biol. Chem. *262*, 5488–5491.

Park, J.B. (2003). Phagocytosis induces superoxide formation and apoptosis in macrophages. Exp. Mol. Med. *35*, 325–335.

Pawelec, G., Derhovanessian, E., and Larbi, A. (2010). Immunosenescence and cancer. Crit. Rev. Oncol. Hematol. *75*, 165–172.

Ponnappan, S., Ovaa, H., and Ponnappan, U. (2007). Lower expression of catalytic and structural subunits of the proteasome contributes to decreased proteolysis in peripheral blood T lymphocytes during aging. Int. J. Biochem. Cell Biol. *39*, 799–809.

Preynat-Seauve, O., Coudurier, S., Favier, A., Marche, P.N., and Villiers, C. (2003). Oxidative stress impairs intracellular events involved in antigen processing and presentation to T cells. Cell Stress Chaperones *8*, 162–171.

Requena, J.R., Chao, C.C., Levine, R.L., and Stadtman, E.R. (2001). Glutamic and aminoadipic semialdehydes are the main carbonyl products of metal-catalyzed oxidation of proteins. Proc. Natl. Acad. Sci. USA *98*, 69–74.

Roberts, C.K., and Sindhu, K.K. (2009). Oxidative stress and metabolic syndrome. Life Sci. *84*, 705–712.

Rodgers, K.J., Hume, P.M., Dunlop, R.A., and Dean, R.T. (2004). Biosynthesis and turnover of DOPA-containing proteins by human cells. Free Radic. Biol. Med. *37*, 1756–1764.

Rudensky, AYu., Preston-Hurlburt, P., Hong, S.C., Barlow, A., and Janeway, C.A., Jr. (1991). Sequence analysis of peptides bound to MHC class II molecules. Nature *353*, 622–627.

Sacksteder, C.A., Qian, W.J., Knyushko, T.V., Wang, H., Chin, M.H., Lacan, G., Melega, W.P., Camp, D.G., 2nd, Smith, R.D., Smith, D.J., et al. (2006). Endogenously nitrated proteins in mouse brain: links to neurodegenerative disease. Biochemistry *45*, 8009–8022.

Sahu, R., Kaushik, S., Clement, C.C., Cannizzo, E.S., Scharf, B., Follenzi, A., Potolicchio, I., Nieves, E., Cuervo, A.M., and Santambrogio, L. (2011). Microautophagy of cytosolic proteins by late endosomes. Dev. Cell *20*, 131–139.

Sharma, S., Dominguez, A.L., and Lustgarten, J. (2006). Aging affect the anti-tumor potential of dendritic cell vaccination, but it can be overcome by co-stimulation with anti-OX40 or anti-4-1BB. Exp. Gerontol. *41*, 78–84.

Shaw, A.C., Joshi, S., Greenwood, H., Panda, A., and Lord, J.M. (2010). Aging of the innate immune system. Curr. Opin. Immunol. *22*, 507–513.

Squier, T.C. (2001). Oxidative stress and protein aggregation during biological aging. Exp. Gerontol. *36*, 1539–1550.

Stadtman, E.R. (1992). Protein oxidation and aging. Science *257*, 1220–1224.

Stadtman, E.R. (2004). Role of oxidant species in aging. Curr. Med. Chem. *11*, 1105–1112.

Starkov, A.A., Fiskum, G., Chinopoulos, C., Lorenzo, B.J., Browne, S.E., Patel, M.S., and Beal, M.F. (2004). Mitochondrial alpha-ketoglutarate dehydrogenase complex generates reactive oxygen species. J. Neurosci. *24*, 7779–7788.

Stern, L.J., Potolicchio, I., and Santambrogio, L. (2006). MHC class II compartment subtypes: structure and function. Curr. Opin. Immunol. *18*, 64–69.

Takahashi, M., Ko, L.W., Kulathingal, J., Jiang, P., Sevlever, D., and Yen, S.H. (2007). Oxidative stress-induced phosphorylation, degradation and aggregation of alpha-synuclein are linked to upregulated CK2 and cathepsin D. Eur. J. Neurosci. *26*, 863–874.

Terman, A. (2006). Catabolic insufficiency and aging. Ann. N Y Acad. Sci. *1067*, 27–36.

Toda, T., Nakamura, M., Morisawa, H., Hirota, M., Nishigaki, R., and Yoshimi, Y. (2010). Proteomic approaches to oxidative protein modifications implicated in the mechanism of aging. Geriatr. Gerontol. Int. *10* (*Suppl 1*), S25–S31.

Tyedmers, J., Mogk, A., and Bukau, B. (2010). Cellular strategies for controlling protein aggregation. Nat. Rev. Mol. Cell Biol. *11*, 777–788.

Wellen, K.E., and Thompson, C.B. (2010). Cellular metabolic stress: considering how cells respond to nutrient excess. Mol. Cell *40*, 323–332.

West, X.Z., Malinin, N.L., Merkulova, A.A., Tischenko, M., Kerr, B.A., Borden, E.C., Podrez, E.A., Salomon, R.G., and Byzova, T.V. (2010). Oxidative stress induces angiogenesis by activating TLR2 with novel endogenous ligands. Nature *467*, 972–976.